# Productivity and Injectivity of Horizontal Wells

DOE/BC/14862--16

**Contract N0. DE-FG22-93BC14862**

RECEIVED
AUG 12 1996
OSTI

Department of Petroleum Engineering
Stanford University
Stanford, CA 94305

Contract Date: March 10, 1993
Anticipated Completion: March 10, 1998

| | |
|---|---|
| Principal Investigator: | Khalid Aziz |
| Co-Investigator: | Thomas A. Hewett |
| Research Associate: | Sepehr Arbabi |
| Administrative Assistant: | Marilyn Smith |
| Technical Project Manager (DOE): | Thomas B. Reid |

Quarterly Report

Reporting Period: April 1, 1996 - June 30, 1996

# Summary of Technical Progress

A number of activities have been carried out in the last three months. A list outlining these efforts is presented below.

- The design and planning of the next phase of the two-phase flow experiments have moved forward. The necessary modifications to allow the use of wire-wrapped screens have been made. The flow loop and the data acquisition system are currently being tested and the new experiments are about to commence.

- Work on obtaining exact well models for a horizontal well or a well of any general profile has continued. A Masters report on this project was completed in June which will be soon submitted to the U.S. DOE as a technical report.

- Work on the application of horizontal wells in gas condensate reservoirs has progressed. The available methods and models are being critically evaluated with the aid of simulation runs.

- Research work on developing coarse grid methods to study cresting in horizontal wells has continued. Correlations for optimum grid size, breakthrough time, and post breakthrough behavior (i.e.; water-oil ratio) are being developed and tested for the problem of water cresting.

- The Ph.D. project on three-dimensional flexible grid simulator (FLEX) was successfully defended in June. The FLEX simulator will be used in future studies as well as in future developments. The dissertation report will be submitted soon to the U.S. DOE.

This quarterly report is based on the last activity listed above. It shows the advantage of our new flexible grid simulator.

# Flexible Grids in Reservoir Simulation (Task 1)

## Case of Aligning Grids Along Streamlines

Streamlines have been used extensively in fluid flow to characterize flow patterns. Thiele et al. [1] presented a novel way of applying streamlines in heterogeneous systems. This example illustrates the alignment of gridblock boundaries along streamlines and the effect of doing this on the water-cut response. The control-volume method [2] can be used to model fluid flow on such grids. Quadrilateral or triangle based flexible grids can be used for this problem. The permeability field used for this example problem is shown in Figure 1. The fine scale permeability is described on a 256 by 128 grid. i.e. 32768 nodes. Permeability varies from 4 mD to 11168 mD. Figure 2 shows the histogram of the permeability distribution.

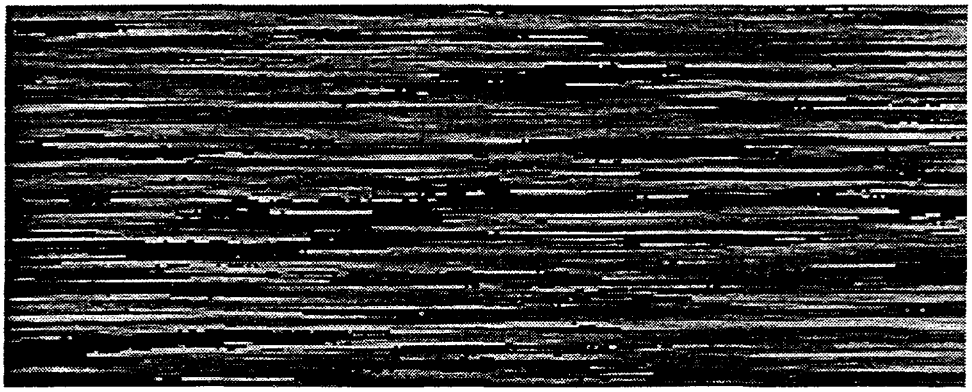

Figure 1: A heterogeneous permeability field

An injector is located on the left side and a producer is located on the right side. Streamlines for constant pressure boundary conditions at both the wells are given in Figure 3.

To simulate the performance of fluid flow in a reasonable time span, this permeability field has to be upscaled. The upscaling procedure can be done along the streamlines. One of the simplest methods of upscaling is to use a power law average. Gridblocks are constructed by aligning the $x$-direction gridblock boundaries along the streamlines. The $y$-direction block boundaries are parallel to the $y$-axis. Since there are a large number of streamlines in the example, streamlines are arbitrarily selected at equal intervals and gridblocks are constrained only to the selected streamlines. The procedure to construct such a grid is given in detail by Verma [3]. An upscaled permeability needs to be calculated for each of the gridblocks. All the fine-scale permeability values which fall inside a gridblock are geometrically averaged.

Four streamline grids are shown in Figures 4 to 7. The underlying upscaled permeability field is also shown in these figures. Dark regions signify higher permeability. The histogram of the upscaled permeability distribution is also shown in these figures.

An injection rate of 100 $m^3/d$ was used for all these examples. Water-cut response at the producer for each of these cases is shown in Figure 8. The figure also shows the reference solution obtained with a commercial simulator, Eclipse. The fine-scale 32768 node grid is used for this reference solution. The reference solution is expected to give the fastest water breakthrough because the water is able to move faster through the high permeability channels of the fine grid. When coarse grids are used, such fine scale variations in permeability are lost through the process of averaging. This results in a more uniform flood-front and hence a later water breakthrough. Alignment of the grid boundaries with the streamlines produces cells with high values in all of the coarsened grids except for the coarsest (140 nodes, see Figure 7). Strictly speaking, representation of the multiphase flow response requires the use of scale averaged relative permeabilities.

The finest upscaled grid used contained 2120 gridnodes. The difference in the 32768 gridblock reference solution and the upscaled 2120 grid problem is not large, considering the fact that the number of gridblocks was reduced by a factor of 16. Even the 540

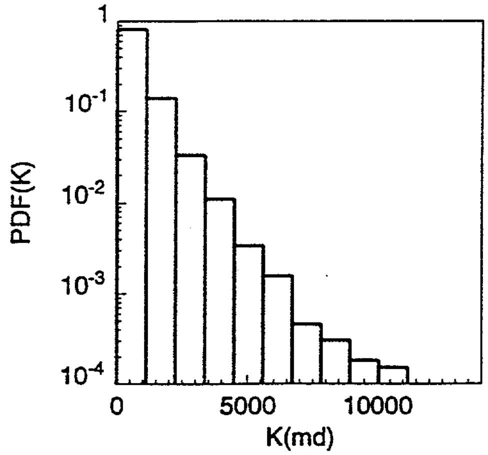


Figure 2: Histogram of permeability distribution

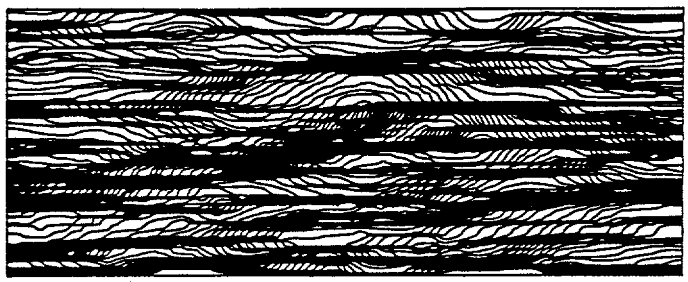

Figure 3: Streamlines for horizontal wells at both ends of Figure 1

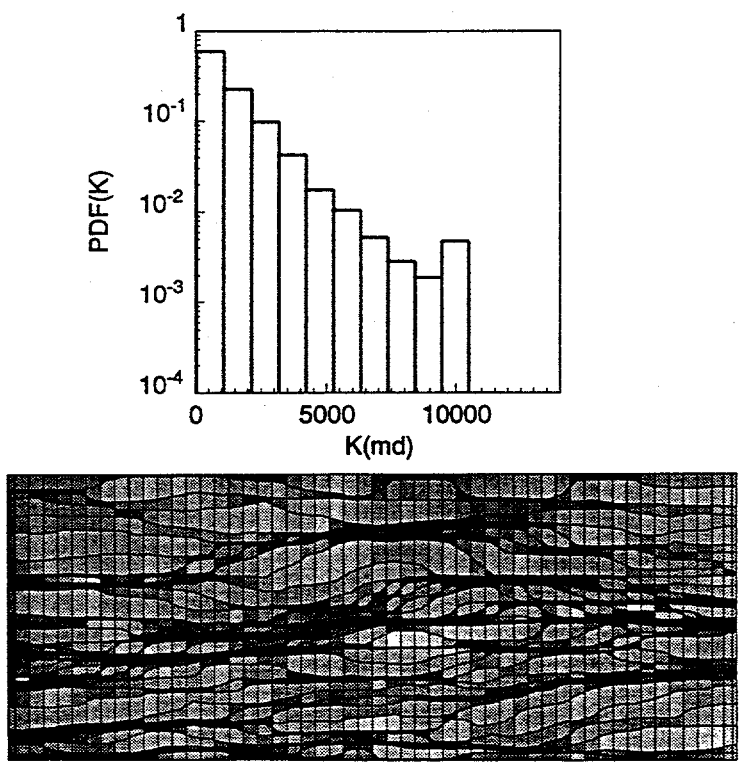


Figure 4: (a) Top: Upscaled permeability distribution for streamline grid with 2120 gridnodes, and (b) Bottom: Streamline grid with 2120 gridnodes.

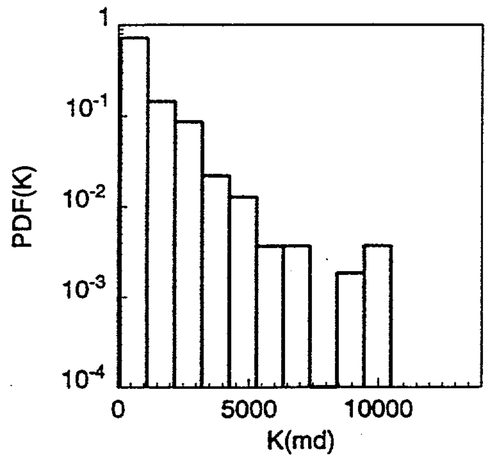


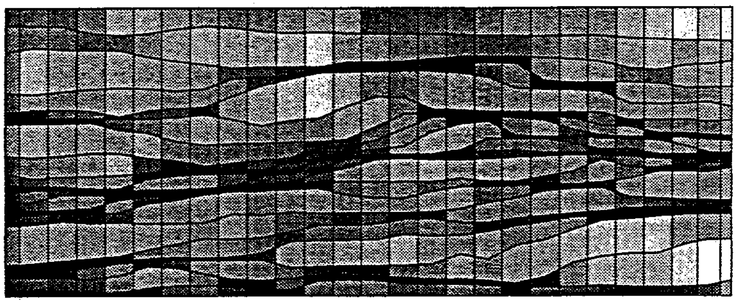

Figure 5: (a) Top: Upscaled permeability distribution for streamline grid with 540 gridnodes, and (b) Bottom: Streamline grid with 540 gridnodes.

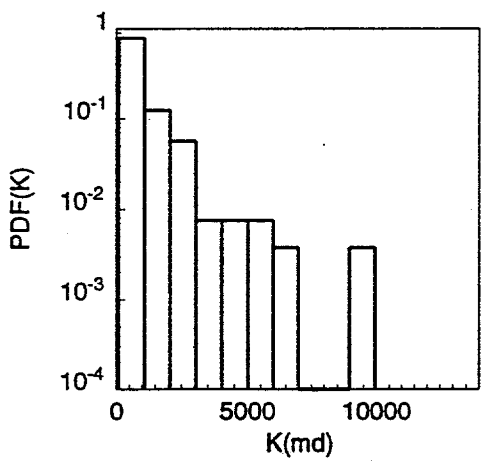


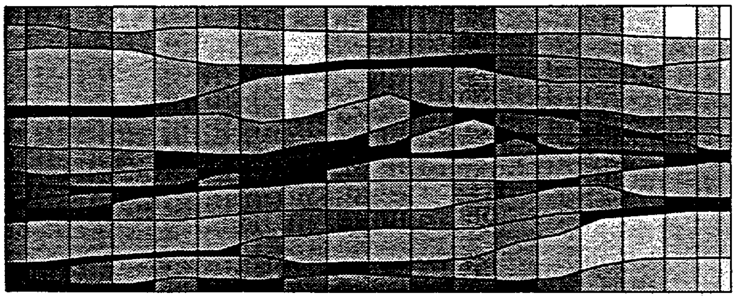

Figure 6: (a) Top: Upscaled permeability distribution for streamline grid with 266 gridnodes, and (b) Bottom: Streamline grid with 266 gridnodes.

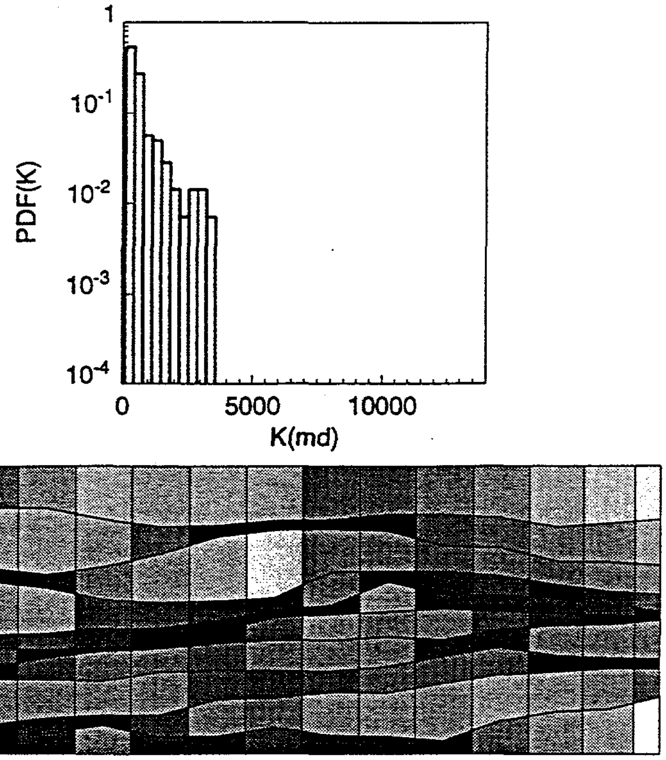


Figure 7: (a) Top: Upscaled permeability distribution for streamline grid with 140 gridnodes, and (b) Bottom: Streamline grid with 140 gridnodes.

gridnode case shows good agreement with the reference solution. This is remarkable considering the fact that the number of gridblocks has been reduced by a factor of about 60. As fewer gridblocks are used, the slope of water-cut response decreases. This is expected due to the upscaling of permeability and the use of the original rock relative permeability curves.

The same problem was also studied with grids that were nót aligned along streamlines. For each of the four cases shown above, normal point-distributed grids were used. The upscaled permeability field for each of these cases is given in Figures 10-12 along with the histogram of upscaled permeability. For the Cartesian grids upscaled permeability, it is observed that the Cartesian grids have less variation in permeability and the higher permeability values are not represented even in the first coarsening of the grid.

The same water flood problem as that for the streamline grid was also run with the Cartesian grids. The water-cut response for each of these cases is shown in Figure 13 along with the water-cut for the streamline grids. It is evident from the figure that aligning the grid block boundaries along streamlines significantly improves the water-cut responses.

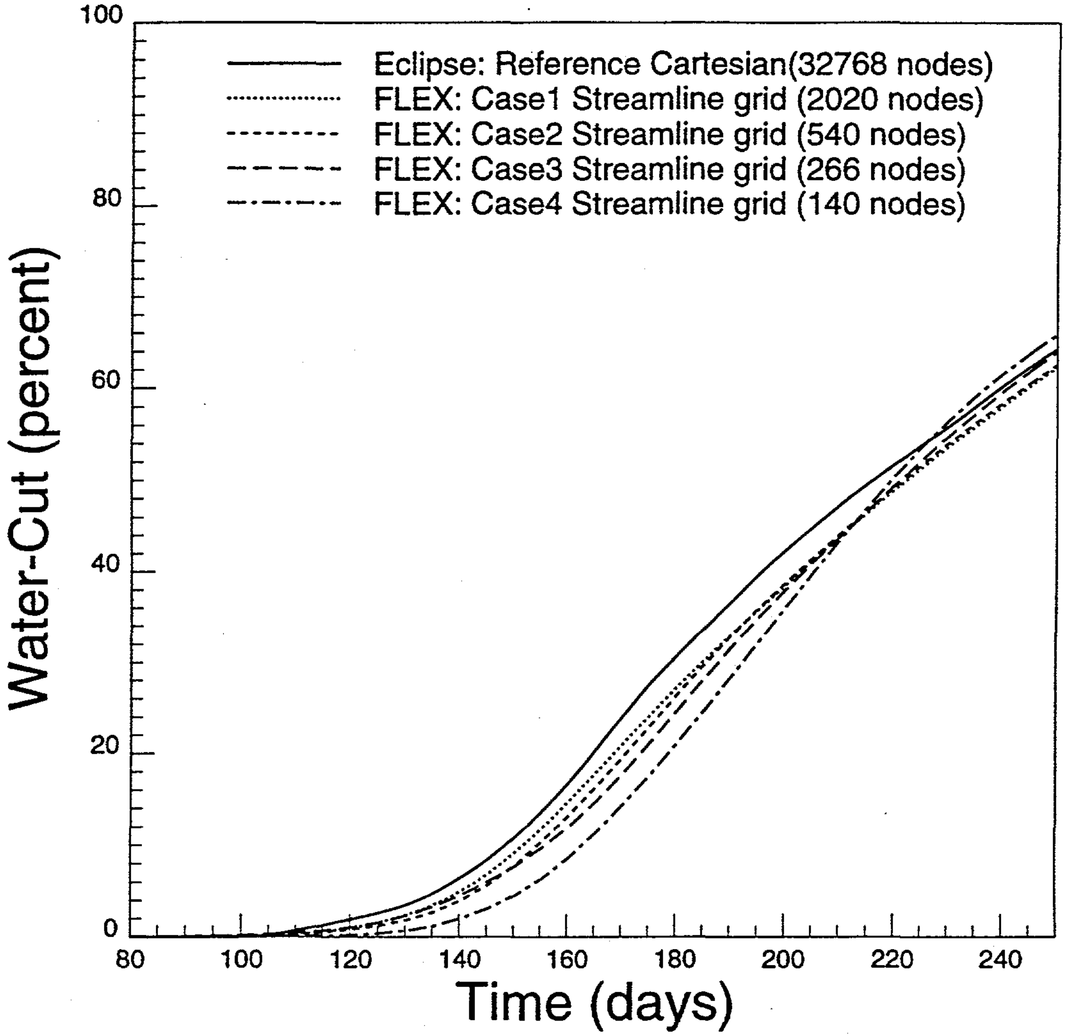


Figure 8: Water-cut of streamline grid compared with fine-scale response

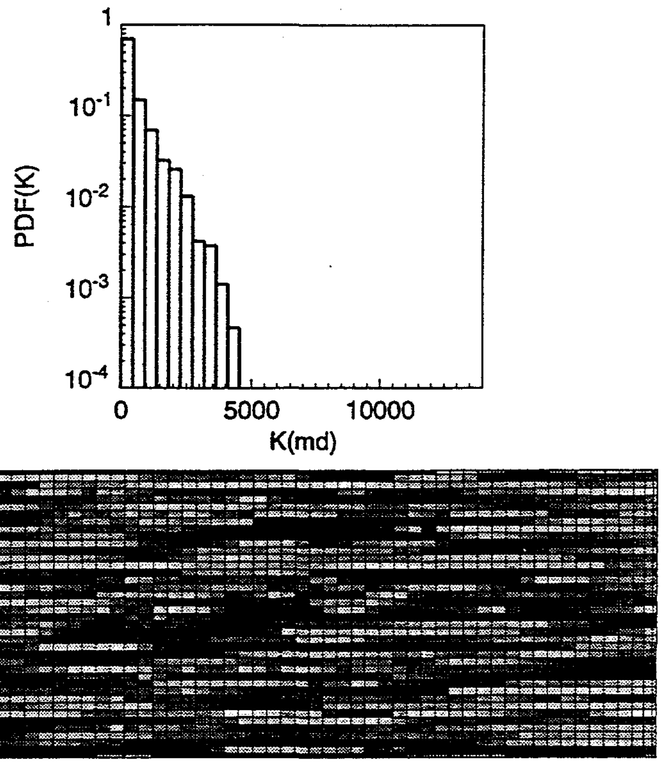


Figure 9: (a) Top: Upscaled permeability distribution for point-distributed Cartesian grid with 2120 gridnodes, and (b) Bottom: Point-distributed Cartesian grid with 2120 gridnodes.

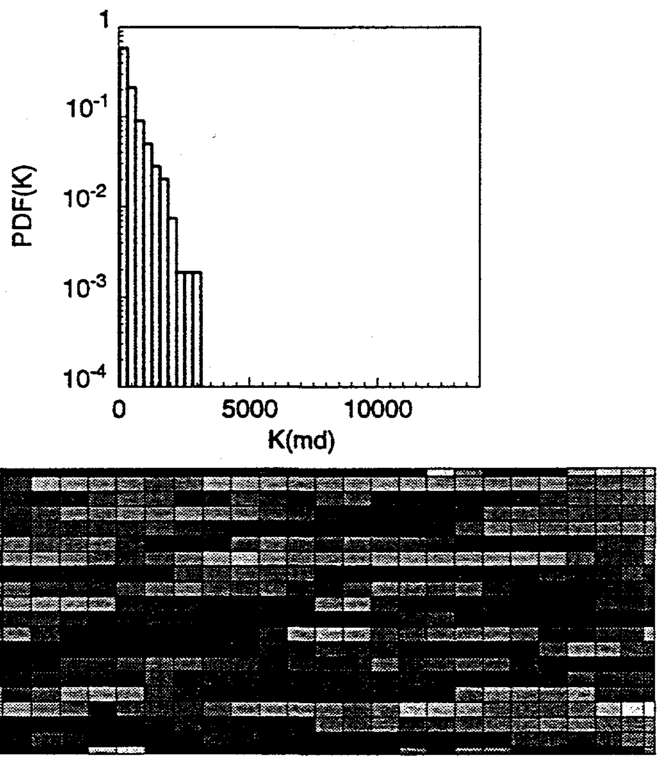


Figure 10: (a) Top: Upscaled permeability distribution for point-distributed Cartesian grid with 540 gridnodes, and (b) Bottom: Point-distributed Cartesian grid with 540 gridnodes.

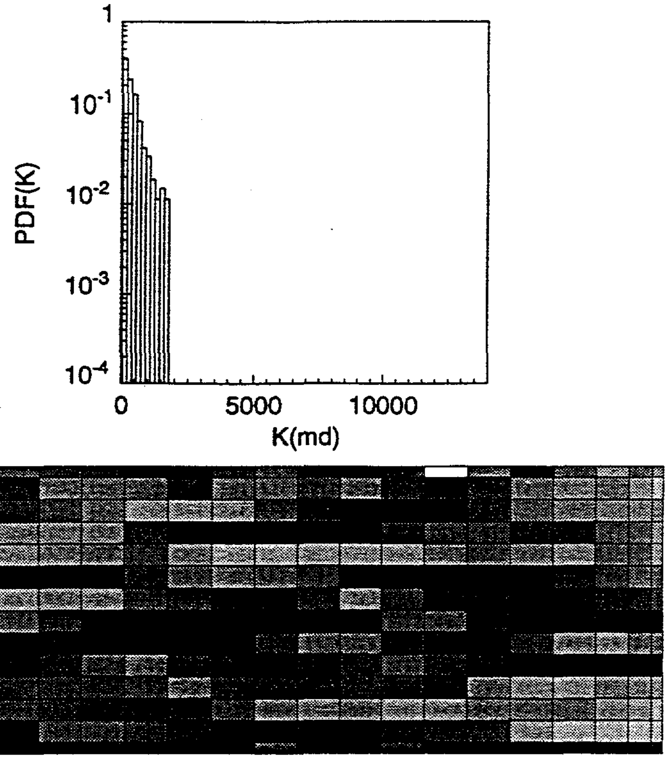


Figure 11: (a) Top: Upscaled permeability distribution for point-distributed Cartesian grid with 266 gridnodes, and (b) Bottom: Point-distributed Cartesian grid with 266 gridnodes.

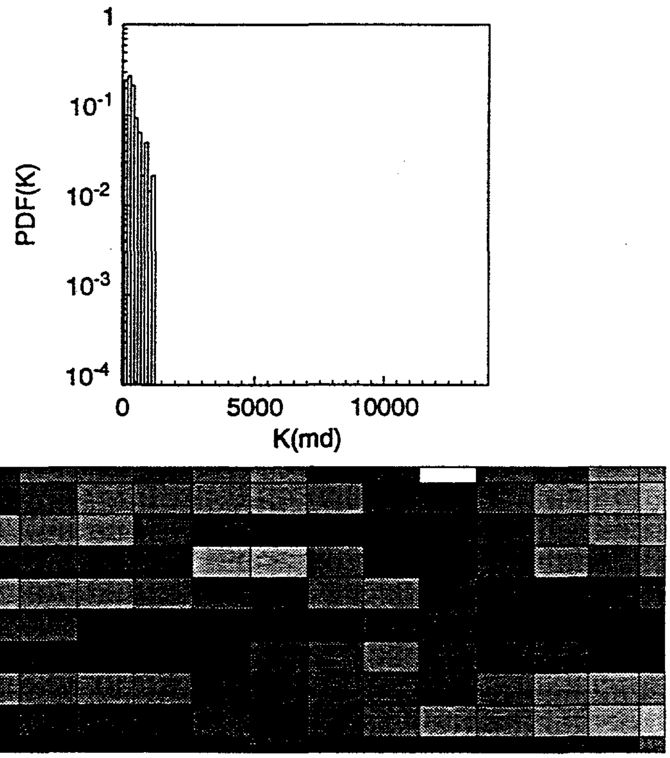


Figure 12: (a) Top: Upscaled permeability distribution for point-distributed Cartesian grid with 140 gridnodes, and (b) Bottom: Point-distributed Cartesian grid with 140 gridnodes.

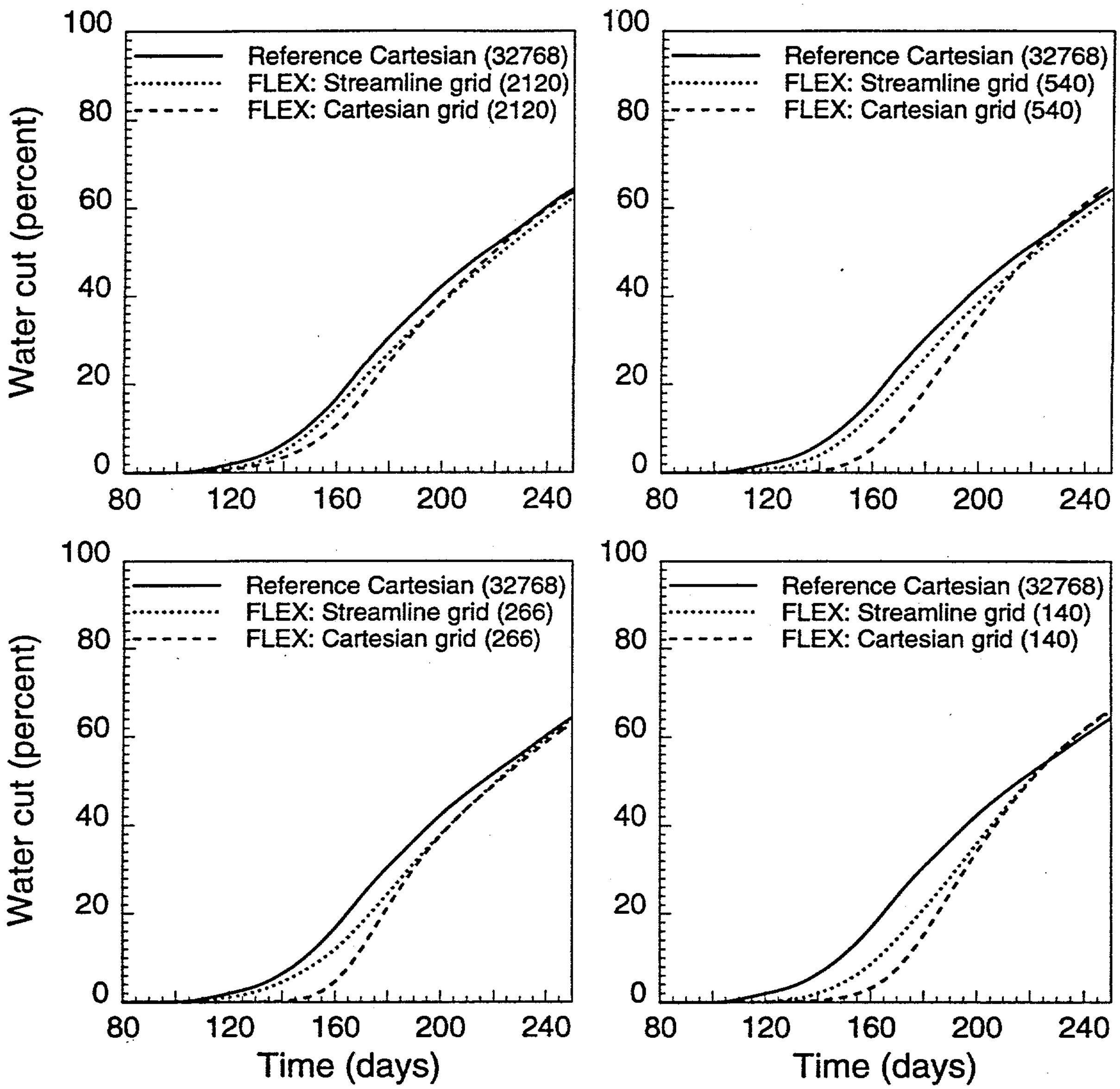


Figure 13: Water-cut response of streamline grid compared with fine-scale and point-distributed Cartesian (a) Top left: 2120 gridnodes (b) Top right: 540 gridnodes (c) Bottom left: 540 gridnodes (d) Bottom right: 140 gridnodes

## References

1. Thiele, M. R., Batycky, R. P., Blunt, M. J. and Orr, F. M.: "Simulating Flow in Heterogeneous Systems Using Streamtubes and Streamlines," *SPERE* (February 1996), **11**, No. 1, 5-12.

2. Verma, S. K.: *Flexible Grids for Reservoir Simulation*, Ph.D. Dissertation, Stanford University, June 1996, chapter 5, 53-94.

3. Verma, S. K.: "The FLEX Manual," Department of Petroleum Engineering, Stanford University, in preparation, (1996).